C26
(Σ26)

ASME - GREEK SECTION, First Nat. Conf. on Recent Advances in Mech. Eng., September 17-20, 2001, Patras, Greece

Proceedings of ASME – Greek Section
September 17-20, Patras, Greece

Paper ANG1/P129

STRESS ANALYSIS OF 3D SOLID STRUCTURES USING LARGE BOUNDARY ELEMENTS DERIVED FROM 2D-*COONS*' INTERPOLATION

Christopher G. Provatidis
National Technical University of Athens
Department of Mechanical Engineering
9 Heroon Polytechniou Avenue, Zografou Campus, GR-157 73 Athens, Greece
Tel: +30-1-7721520, Fax: +30-1-7722347
E-mail: prowaton@central.ntua.gr

ABSTRACT

This paper proposes a new technique to improve the efficiency of the Boundary Element Method so that to become capable of drastically reducing the number of collocation points involved. The method refers to an elastic solid structure of arbitrary shape, consisting of several curvilinear boundary patches. For each patch the new method applies the well-known Coons' interpolation formula, which is the simplest mathematical representation of a surface in Computational Geometry. By using Coons' formula, all three: geometry, boundary displacements and tractions are interpolated in terms of their values along the edges of the patch in which they belong. As a result, no degrees of freedom appear within the patches excepting their edges. Since the involved geometrical entities can be the absolutely necessary quantities that built-up the CAD-model, the proposed method seems to "marry" CAD with CAE. The efficiency of the method is elucidated with three numerical examples.

KEYWORDS

Boundary Element Method, CAD, CAE, Coons' interpolation, Stress analysis.

INTRODUCTION

Thirty-four years after the first practical application of the Boundary Element Method (BEM) in stress analysis by Rizzo [1], it is now a well-established technique. The key ingredient is to apply the historical Somigliana's [2] integral equations in conjunction with constant, linear or quadratic interpolation of both the displacements and tractions along the boundary of a solid structure [3, 4]. The advantage of BEM is that it reduces the dimensionality of the problem by one; from 3D (volume) to 2D (surface). This paper investigates the possibility of using as less boundary information as possible and achieves to reduce the dimensionality of the problem by one more; from 3D (structure's volume) to 1D (lines of the patches).

NOMENCLATURE

V	volume of the structure
K_{ip}	number of nodes in the whole structure
N_l	number of points on patch boundary
N_n	total number of nodes in the whole structure
N_p	number of patches in the structure
b_i	body force
ip	ascending number of a patch
p_k	traction
u_k	boundary displacement
u^*_{lk}	fundamental solution
Γ	boundary of the structure
Φ_k	global shape functions

ξ, η normalized co-ordinates

σ_{ij} stress tensor

THE GENERAL CONCEPT

In stress analysis problems the objective purpose is to solve equilibrium equations that are written in tensor form as

$$\partial \sigma_{ij} / x_j + b_i = 0 \tag{1}$$

A solution of Eq. (1) can be derived by applying BEM, characterized by the well-known integral equation [3,4]

$$c^i u_l^i + \oint\!\!\oint_\Gamma p_{lk}^* u_k \, d\Gamma = \oint\!\!\oint_\Gamma u_{lk}^* p_k \, d\Gamma + \int_V u_{lk}^* b_k \, dV \tag{2}$$

As it can be noticed, in Eq. (2) only boundary integrals are involved, excepting the body forces. The advantage of BEM is that it reduces the dimensionality of the problem by one; from 3D (volume) to 2D (surface) integrals. The common practice is to solve Eq. (2) in conjunction with constant, linear or quadratic interpolation of both the displacements u_k and tractions p_k along the boundary of a solid structure [3, 4].

In order to interpolate u_k and p_k in a more efficient way, let us assume that the solid structure under consideration is made of large surface patches. Let us also assume that over each patch the variation of both boundary displacements and tractions is adequately smooth (not an abrupt change occurs). The novel idea of this paper is to interpolate both boundary displacements and tractions within each patch by applying a global set of cardinal functions instead of dividing all surfaces in small boundary elements. In this way, the number of degrees of freedom is drastically reduced.

The global interpolation is performed as follows. Within each patch the displacements and tractions are expressed with respect to nodal points arranged along the four (or three) surrounding edges. As a result, the nodal points and the associated degrees of freedom appear only along the edges of the boundary.

GLOBAL INTERPOLATION

In the proposed method, the boundary displacement vector $\mathbf{u}(x, y, z)$ inside a patch is approximated by:

$$\mathbf{u}(\xi,\eta) = \sum_{k=1}^{K} \mathbf{\Phi}_k(\xi,\eta)\mathbf{u}_k \tag{3}$$

with $\Phi_k(\xi,\eta)$ denoting the global shape function, $\mathbf{u}_k$ nodal degrees of freedom appearing only at the boundaries of the patch, while ξ and η being its normalised $(0 \le \xi, \eta \le 1)$ curvilinear co-ordinates. Dependent on the type of the patch under consideration, two cases are distinguished.

I. Four-sided patch

Following Coons [5], the co-ordinates of a point $\mathbf{x}(\xi,\eta)$ inside a four-sided patch can be expressed in a closed analytical form in terms of its four "boundaries" ξ = 0,1 and η = 0,1: $\mathbf{x}(0,\eta)$, $\mathbf{x}(1,\eta)$, $\mathbf{x}(\xi,0)$, $\mathbf{x}(\xi,1)$:

$$\begin{aligned}\mathbf{x}(\xi,\eta) = {} & (1-\xi)\,\mathbf{x}(0,\eta) + \xi\,\mathbf{x}(1,\eta) + (1-\eta)\,\mathbf{x}(\xi,0) + \eta\,\mathbf{x}(\xi,1) \\ & -(1-\xi)(1-\eta)\,\mathbf{x}(0,0) - \xi(1-\eta)\,\mathbf{x}(1,0) \\ & -(1-\xi)\eta\,\mathbf{x}(0,1) - \xi\eta\,\mathbf{x}(1,1)\end{aligned} \tag{4}$$

In this paper it is assumed that displacement **u** inside the patch are also implemented in a similar way, as follows:

$$\begin{aligned}\mathbf{u}(\xi,\eta) = {} & E_0(\xi)\,\mathbf{u}(0,\eta) + E_1(\xi)\,\mathbf{u}(1,\eta) \\ & + E_0(\eta)\,\mathbf{u}(\xi,0) + E_1(\eta)\,\mathbf{u}(\xi,1) \\ & - \sum_{i=0}^{1}\sum_{j=0}^{1} E_i(\xi)\,E_j(\eta)\,\mathbf{u}(\xi_i,\eta_j)\end{aligned} \tag{5}$$

The "blending" functions shown in Figure 1 are given as

$$E_0(\eta) = 1-\eta, \; E_1(\eta) = \eta \tag{6}$$

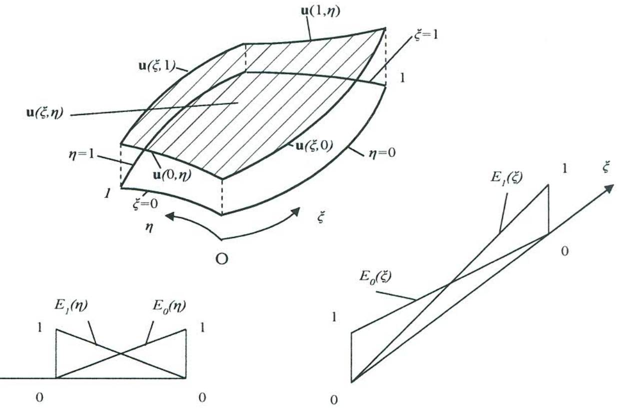

Fig. 1: Boundary curves $\mathbf{u}(0,\eta)$, $\mathbf{u}(1,\eta)$, $\mathbf{u}(\xi,0)$, $\mathbf{u}(\xi,1)$ and 'blending functions' E_0 and E_1 of the patch.

II. Three-sided patch

The co-ordinates of a point $\mathbf{x}(\xi,\eta)$ inside a three-sided patch can be also expressed in a closed analytical form in terms of its "boundaries". The interested reader may consult Barnhill et al. [6-8].

This paper extends the idea of Kanarachos [9-12] applied in two-dimensional FEM analysis, where the displacement had been interpolated within the patch using Eq. (5), and applies it here for the tractions, too. In both configurations, four- or three-sided patch, the next step will be to determine a suitable discretization scheme along the boundaries of the patch. Having prescribed $3q$ (different) degrees of freedom ($3q$

nodes) an each boundary, $\mathbf{u}(0,\eta_i)$, $\mathbf{u}(1,\eta_i)$, $\mathbf{u}(\xi_i,0)$, $\mathbf{u}(\xi_i,1)$, i=1,2,...,q, appropriate interpolating formulae for the functions $\mathbf{u}(0,\eta)$, $\mathbf{u}(1,\eta)$, $\mathbf{u}(\xi,0)$ and $\mathbf{u}(\xi,1)$ are sought. Considering that q may be allowed to be a large number, a Lagrangian interpolation polynomial would tend to produce undesirable oscillations between two arbitrary abscissae η_i and η_{i+1}, as it may possess as many as (q-1) maxima and minima over its entire interval of variation. For this reason, the use of splines is envisaged:

Given q degrees of freedom on the boundary of the patch at $n_1, n_2, \ldots, n_q$ a spline function $B(n)$ of degree m is a function having the two following properties[9]:

(1) In each interval (n_i, n_{i+1}), i=1, 2, ..., q-1, $B(n)$ is given by a polynomial of degree m or less.

(2) $B(n)$ and its derivatives of order 1, 2, ..., m-1 are continuous everywhere.

A commonly used spline function is the truncated power function $\langle n-n_i\rangle^m$, for any variable n-n_i and for any positive integer m. This function is defined by:

$$\begin{aligned} \langle n-n_i\rangle^m &= (n-n_i)^m \quad , \quad for\ n-n_i > 0; \\ \langle n-n_i\rangle^m &= 0 \quad , \quad for\ n-n_i < 0 \end{aligned} \tag{7}$$

It is easily seen that the function $B(n)$ has a unique representation of the form:

$$\begin{aligned} B(n) &= b_0 + b_1 n + b_2 n^2 + \ldots + b_{m-1} n^{m-1} \\ &\quad + \sum_{i=1}^{q-1} a_i \langle n-n_i\rangle^m \\ &= P(n) + \sum_{i=1}^{q-1} a_i \langle n-n_i\rangle^m \end{aligned} \tag{8}$$

with $P(n)$ denoting a polynomial of degree (m-1) and a_i properly chosen constants. The most common case is that the spline of order m = 4 (degree 3), that is of cubic B-splines. If now $B_j(n)$, where n is either r or s, denote cardinal splines of degree m, then the functions $\boldsymbol{u}(0, s)$, $\boldsymbol{u}(1, s)$, $\boldsymbol{u}(r, 0)$ and $\boldsymbol{u}(r, 1)$ could be written in the following form:

$$\begin{aligned} &\mathbf{u}(0,s) = \sum_{j=1}^{q} B_j(\eta)\mathbf{u}(0,\eta_j) \quad \mathbf{u}(1,\eta) = \sum_{j=1}^{q} B_j(\eta)\mathbf{u}(1,\eta_j) \\ &\mathbf{u}(\xi,0) = \sum_{j=1}^{q} B_j(\xi)\mathbf{u}(\xi_j,0) \quad \mathbf{u}(\xi,1) = \sum_{j=1}^{q} B_j(\xi)\mathbf{u}(\xi_j,1) \end{aligned} \tag{9}$$

which, when substituting in Eq. (5), determines the global shape functions $\Phi_k(\xi,\eta)$ involved in Eq. (3).

NUMERICAL PROCEDURE

The co-ordinate vector within the patch is interpolated on the basis of the boundaries of the patch as follows

$$\mathbf{x}(\xi,\eta) = \sum_{j=1}^{N_l} \Phi_j(\xi,\eta)\mathbf{x}_i^j = \mathbf{\Phi x} \tag{10}$$

It is also considered that both the displacement and traction vectors at a point $P(\xi,\eta)$ within the patch are interpolated in the same manner (isoparametric macro-element)

$$\begin{aligned} \mathbf{u}(\xi,\eta) &= \sum_{j=1}^{N_l} \Phi_j(\xi,\eta)\mathbf{u}_i^j = \mathbf{\Phi u} \\ \mathbf{p}(\xi,\eta) &= \sum_{j=1}^{N_l} \Phi_j(\xi,\eta)\mathbf{p}_i^j = \mathbf{\Phi p} \end{aligned} \tag{11}$$

By substituting Eq. (11) in Eq. (2) one obtains

$$\begin{aligned} c^i\mathbf{u}^i &+ \sum_{ip=1}^{Np}\left\{\oint_{\Gamma_{ip}} \mathbf{p}_{lk}^* \mathbf{\Phi}_k \, d\Gamma\right\}\mathbf{u}_{ip} \\ &= \sum_{ip=1}^{Np}\left\{\oint_{\Gamma_{ip}} \mathbf{u}_{lk}^* \mathbf{\Phi}_k \, d\Gamma\right\}\mathbf{p}_{ip} \end{aligned} \tag{12}$$

Equation (12) can be written for each node "Ip" out of the N_p total nodes as follows

$$\begin{aligned} c^i\mathbf{u}^i &+ \sum_{ip=1}^{Np}\left\{\int_{ip} \mathbf{p}_{lk}^* \mathbf{\Phi}_k(\xi,\eta)|G(\xi,\eta)|\, d\xi\, d\eta\right\}\mathbf{u}_{ip} \\ &= \sum_{ip=1}^{Np}\left\{\int_{ip} \mathbf{u}_{lk}^* \mathbf{\Phi}_k(\xi,\eta)|G(\xi,\eta)|\, d\xi\, d\eta\right\}\mathbf{p}_{ip} \end{aligned} \tag{13}$$

where the Jacobian is given by

$$\begin{aligned} |G| &= \left(g_1^2 + g_2^2 + g_3^2\right)^{1/2} \\ g_1 &= \frac{\partial x_2}{\partial \xi}\frac{\partial x_3}{\partial \eta} - \frac{\partial x_2}{\partial \eta}\frac{\partial x_3}{\partial \xi} \\ g_2 &= \frac{\partial x_1}{\partial \xi}\frac{\partial x_3}{\partial \eta} - \frac{\partial x_1}{\partial \eta}\frac{\partial x_3}{\partial \xi} \\ g_3 &= \frac{\partial x_1}{\partial \xi}\frac{\partial x_2}{\partial \eta} - \frac{\partial x_1}{\partial \eta}\frac{\partial x_2}{\partial \xi} \end{aligned} \tag{14}$$

Now, for the purposes of the numerical integration only, the patch is divided into $N_\xi \times N_\eta$ cells where a second set of normalized co-ordinates $(-1 \le \xi', \eta' \le 1)$ is introduced, as shown in Fig. 2. So, the term $|G(\xi,\eta)|d\xi\, d\eta$ in Eq. (13) is replaced by $|G(\xi,\eta)\cdot G'(\xi',\eta')|d\xi' d\eta'$, which requires a trivial (e.g., $2\times 2, 3\times 3, 4\times 4$) Gaussian quadrature.

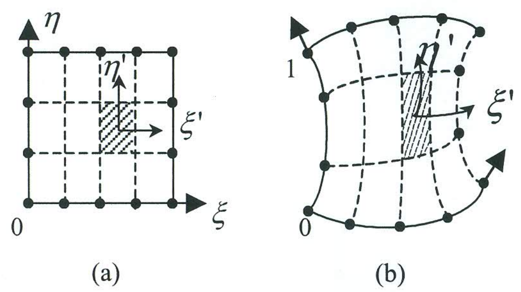

Fig. 2 (a) Unit reference and (b) Real patch geometry.

So, the final algebraic system obtains the form

$$\mathbf{C\,U} + \sum_{ip=1}^{Np} \mathbf{H}^{ip}\,\mathbf{U}^{ip} = \sum_{ip=1}^{Np} \mathbf{G}^{ip}\,\mathbf{P}^{ip} \tag{15}$$

where $\mathbf{U}$ is the displacement vector of all nodes on the boundary of the structure (along the patch edges), $\mathbf{U}^{ip}$ and $\mathbf{P}^{ip}$ are displacement and traction vectors referring to the *ip*-th patch. Also, the matrices $\mathbf{H}^{ip}$ and $\mathbf{G}^{ip}$ are of order $3N_n \times 3K_{ip}$, where N_n is the number all nodes of the whole structure and K_{ip} is the number of the *ip*-th patch. Their elements $\mathbf{H}_{ij}^{ip}$ and $\mathbf{G}_{ij}^{ip}$, each of order 3x3, relate the *i*-th geometrical node of the structure with the *j*-th node of the *ip*-th patch. The $\mathbf{C}$-matrix is a diagonal one of order $3N_n \times 3N_n$.

It is here reminded that apart of the particular case of an ideal smooth boundary, in most cases the number of the geometry nodes is smaller than the number N_m of traction points [4]. So, Eq. (15) finally becomes

$$\mathbf{C\,U} + \hat{\mathbf{H}}\,\mathbf{U} = \mathbf{G\,P} \tag{16}$$

where

$\mathbf{C}$	: diagonal matrix ($3N_n \times 3N_n$)
$\mathbf{U}$	: displacement vector ($3N_n \times 1$)
$\mathbf{P}$	: traction vector ($3N_m \times 1$)
$\hat{\mathbf{H}}$	: total displacement –influence matrix ($3N_n \times 3N_n$)
$\mathbf{G}$	: total traction-influence matrix ($3N_n \times 3N_m$)

Again, the final displacement–influence matrix ($\hat{\mathbf{H}}$) is square while the traction–influence one ($\mathbf{G}$) will be nonsquare possessing more columns than rows.

With respect to the diagonal terms of the matrix $\mathbf{H} = \mathbf{C} + \hat{\mathbf{H}}$, these can be easily calculated as in the conventional BEM [3, 4] on the basis of rigid body considerations. In this work, no special attention was given to the singular $\mathbf{G}_{ii}$-terms.

NUMERICAL EXAMPLES

The proposed method is sustained by three examples.

Example 1: Cube in tension

A cube of unit length is fixed at its one surface (x_1=0) while the opposite side is uniformly loaded in tension (P_x=1). Elastic modulus and Poisson's ratio are: E=1, v=0.

This problem was solved for three different uniform meshes of twenty, forty-four and sixty-four geometry (displacement) nodes, respectively, as shown in Fig. 3.

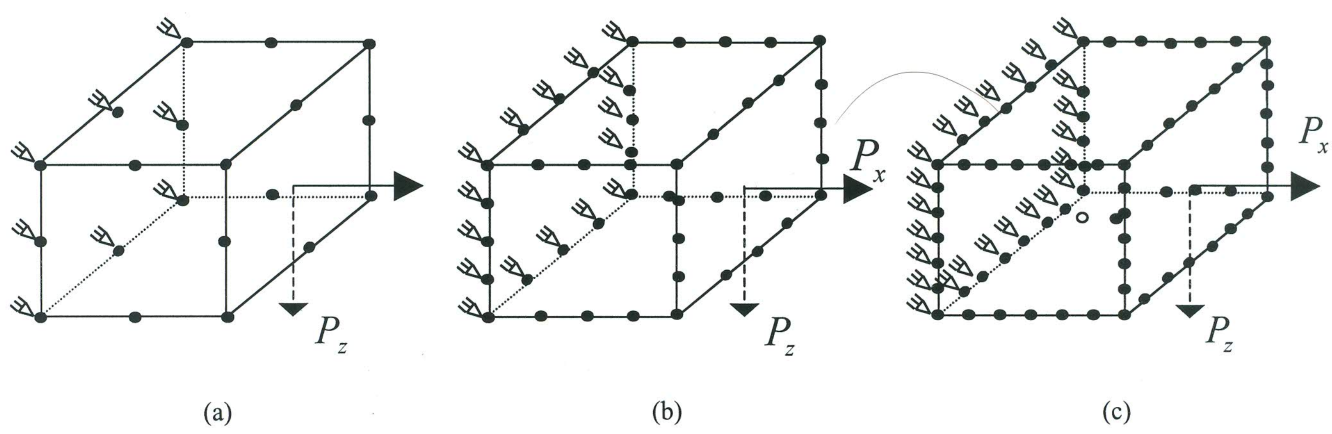

Fig. 3 Clamped unit cube model using (a) twenty, (b) forty-four and (c) sixty-four nodes, uniformly distributed

Each case was also solved for three different Gaussian quadratures: 2x2, 3x3 and 4x4 per cell. Results are presented in Table 1.

Table 1 Calculated displacement at the loaded surface: Tension

Number of nodes	Gauss points per cell			Exact solution
	2×2	3×3	4×4	
20	0.939	0.972	0.984	1.000
44	0.978	0.989	0.994	1.000
68	0.989	0.994	0.997	1.000

Example 2: Cube in bending

A cube of unit length is fixed at its one surface (x_1=0) while the opposite side is loaded by a uniform shear traction in bending (P_z=3.2). Elastic modulus and Poisson's ratio are: E=1, ν=0.2. This problem was solved for a uniform mesh of forty-four geometry (displacement) nodes (Fig. 3b) using three different Gaussian quadrature schemes: 2×2, 3×3 and 4×4 per cell. As only approximate closed formulas exist for this example, now the results shown in Table 2 are compared with the commercial FEM-code ALGOR (for the same number of divisions).

Table 2 Calculated displacement at the loaded surface: Bending

Displacement	Gauss points per cell			ALGOR
	2×2	3×3	4×4	
u	9.53	10.06	10.25	10.13
v	0.00	0.00	0.00	0.00
w	20.18	21.14	21.49	21.35

Example 3: Thick hollow cylinder under internal pressure.

A thick hollow cylinder (R_i=10mm, R_e=20mm) and height L=20 mm is subjected to a uniform internal pressure P=20 MPa. The model consists of one-fourth (90 degrees) circumferentially where lower and upper sides do not move alond the axis of revolution but they only roll on the plane (x_1,x_2) shown in Fig. 4. The material is isotropic and linear elastic (E=210000 MPa, ν=0.3).

The numerical model consists of forty-four geometry (displacement) nodal points. In other words it consists of six patches with sixteen nodes per patch. Numerical results are presented at boundary nodes (Tables 3 and 4) as well as at internal points. In all cases these are compared with the analytical solution given as

$$\sigma_\theta = \frac{a^2 P}{b^2 - a^2}\left(1 + \frac{b^2}{r^2}\right) , \quad \sigma_r = \frac{a^2 P}{b^2 - a^2}\left(1 - \frac{b^2}{r^2}\right)$$

$$E\varepsilon_\theta = \sigma_\theta - \nu\sigma_r , \quad \varepsilon_\theta = \frac{u}{r} , \quad u = \frac{r}{E}(\sigma_\theta - \nu\sigma_r)$$

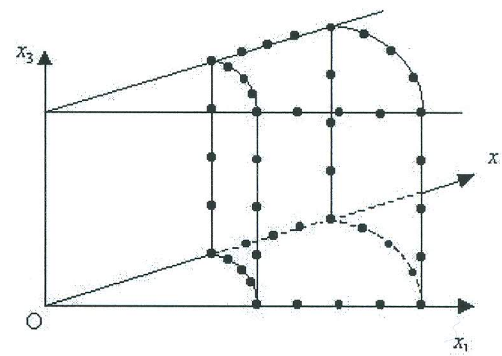

Fig. 4 One-fourth of a thick cylinder

Boundary nodes

Table 3 Radial displacement ($u_r \times 10^3$) on the internal boundary

2×2	3×3	4×4	Exact
1.79	1.83	1.85	1.87

Table 4 Circumferential stresses σ_θ (MPa) on the boundary

2×2	3×3	4×4	Exact
-36.10	-34.58	-34.28	-33.33

Internal nodes

Table 5 Radial displacement ($u_r \times 10^3$) in the interior at x_3=L/2=10

Radius (R)	Gauss points per cell			Exact
	2×2	3×3	4×4	
12.5	1.60	1.56	1.57	1.59
15.0	1.38	1.39	1.41	1.43
17.5	1.31	1.32	1.31	1.33

Table 6 Circumferential stresses σ_θ (MPa) in the interior at $x_3 = L/2 = 10$

Radius (R)	Gauss points per cell			Exact
	2×2	3×3	4×4	
12.5	24.92	24.30	23.41	23.73
15.0	17.35	18.07	18.26	18.52

DISCUSSION

A characteristic of the proposed method is that it leads to reliable results even for a few number of boundary nodes. Moreover, a small increase in accuracy appears when increasing the number of boundary nodes and/or the number of integration points per cell.

The criterion of choosing the frontiers of the involved patches is related to their geometrical smoothness as well as to the absence of any abrupt changes in the related boundary conditions.

Finally, it should be mentioned that in all examples of this paper, the boundary is composed of six discrete patches, which constitute a generalized curvilinear paralleloid. This paralleloid was analyzed by using only its twelve edges. Again, only the boundary data, which are absolutely necessary for the development of the CAD (geometry) model, were involved in the analysis. In this sense, the proposed method seems to "marry" CAD with CAE.

CONCLUSIONS

A new method was proposed for the development of large boundary elements that are extended over a significant part of the boundary. The background is the application of Coons' interpolation formula in conjunction with B-splines. The method was tested in elastostatic analysis and was found to converge fast and be reliable even for a small number of nodal points.

REFERENCES

[1] Rizzo, F. J., 1967, "An integral equation approach to boundary value problems of classical elastostatics," Q. Appl. Math., **25** (3)

[2] Somigliana, C., 1886, "Sopra l'equilibrio di un corpo elastico isotropo," Il Nuovo Ciemento, pp. 17-19.

[3] Brebbia, C. A., 1978, The Boundary Element Method for engineers, Pentech Press, London.

[4] Banerjee, P. K., and Butterfield, R., 1981, Boundary Element Methods in Engineering Science, McGraw-Hill, London.

[5] Coons, S. A., 1967, "Surfaces for computer aided design of space form," Technical report MAC-TR-41, MIT. Available by CFSTI, Sills Building, 5285 Port Royal Road, Springfield, Virginia 22151, U.S.A.

[6] Barnhill, R. E., and Gregory, J. A., 1975, "Compatible smooth interpolation on triangles," J. Approx. Theory, **15**, pp. 214-225

[7] Barhill, E., and Mansfield, L., 1974, "Error bounds for smooth interpolation on triangles," J. Approx. Theory, **11**, pp. 306-318

[8] Barhill, E., Birkhoff, G., and Gordon, M. J., 1973, "Smooth interpolation on triangles," J. Approx. Theory, **8**, pp. 114-128

[9] Kanarachos, A., and Deriziotis, D., 1989, "On the solution of Laplace and wave propagation problems using C-elements," Finite Element in Analysis and Design, 5, pp. 97-109.

[10] Kanarachos, A., Provatidis, Ch, Deriziotis, D., and Foteas, N., 1999, "A new approach of the fem analysis of two-dimensional elastic structures using global (Coons's) interpolation functions,", European Conference on Computational Mechanics, Wunderlich J, editor, CD Proceedings.

[11] Provatidis, Ch., and Kanarachos, A., "On the use of Coons' interpolation in CAD/CAE systems," MCME 2000: 2nd Int. Conference on Mathematics and Computers in Mechanical Engineering, Vouliagmeni, Greece.

[12] Kanarachos, A., Grekas, D., Provatidis, Ch., 1995, "Generalized Formulation of Coons' Interpolation", In: P. Kaklis and S. Sapidis (eds.), Computer Aided Geometric Design: From Theory to Practice, National Technical University of Athens, Chapter 7, pp. 65-76.